

Entropy-Based Rational Modulation of the pK_a of a Synthetic pH-Dependent Nanoswitch

Davide Mariottini,[†] Andrea Idili,[†] Minke A. D. Nijenhuis,[‡] Gianfranco Ercolani,[†] and Francesco Ricci^{*,†}

[†]Chemistry Department, University of Rome, Tor Vergata, Via della Ricerca Scientifica, 00133 Rome, Italy

[‡]Interdisciplinary Nanoscience Center (iNANO), Aarhus University, DK-8000 Aarhus C, Denmark

Supporting Information

ABSTRACT: The rational regulation of the pK_a of an ionizable group in a synthetic device could be achieved by controlling the entropy of the linker connecting the hydrogen bond forming domains. We demonstrate this by designing a set of pH-responsive synthetic DNA-based nanoswitches that share the same hydrogen bond forming domains but differ in the length of the linker. The observed acidic constant (pK_a) of these pH-dependent nanoswitches is linearly dependent on the entropic cost associated with loop formation and is gradually shifted to more basic pH values when the length of the linker domain is reduced. Through mathematical modeling and thermodynamic characterization we demonstrate that the modulation of the observed pK_a is due to a purely entropic contribution. This approach represents a very versatile strategy to rationally modulate the pK_a of synthetic devices in a highly predictable and accurate way.

Hydrogen bonds are ubiquitous in nature and represent one of the most important interactions in life.^{1–5} Among the many advantages associated with hydrogen bonding such as reversibility, synthetic accessibility, and directionality,⁶ another feature makes this chemical interaction extremely appealing: its dependence on pH is highly tunable. The pK_a of an ionizable group in a protein, for example, can shift by several pH units due to changes in the surrounding microenvironment.⁷

For the above characteristics, hydrogen bonds are also among the most utilized noncovalent interactions used to design and build supramolecular assemblies,^{6,8,9} polymers,^{10–12} multifunctional materials,¹³ mechanically interlocked molecular architectures,^{14–17} and pH-responsive devices.^{18–21} Despite this extensive use, however, the possibility to tune the pK_a of ionizable groups in synthetic systems with the same efficiency found in proteins has proven extremely difficult. Examples have demonstrated the possibility to control the pK_a of supramolecular systems by photochemical²² or electrochemical²³ inputs or by complexation,²⁴ but the modulation of pK_a remains difficult to predict and to achieve in a rational way.

Motivated by the above arguments, here we demonstrate that rational regulation of the pK_a of an ionizable group in a synthetic device could be achieved through the design of intrinsically disordered regions connecting the hydrogen-bond forming domains (Figure 1). By doing so we show that

through a purely entropic contribution it is possible to modulate the pK_a of ionizable groups in a highly versatile and predictable way.

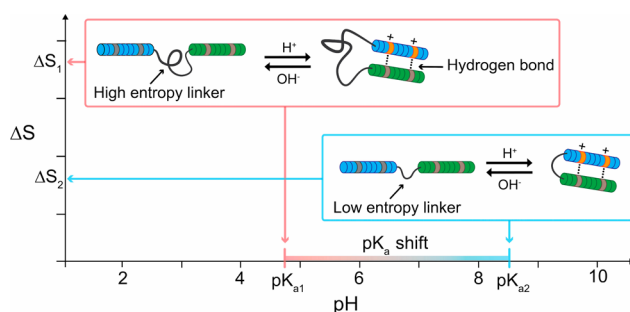


Figure 1. Observed acidic constant (pK_a) of a pH-dependent synthetic switch can be rationally tailored by modulating the length of the linker domain that connects the portions undergoing hydrogen bonds (dotted line). When a lower entropic cost is associated with loop formation, the observed pK_a of the switch is shifted to more basic pH values.

To achieve this goal, we took advantage of the high programmability of DNA interactions^{25–27} and we designed a pH-responsive nucleic acid nanoswitch (Figure 2) that can form an intramolecular triplex structure through hydrogen bonds (Hoogsteen interactions) between a hairpin duplex domain and a single-strand triplex-forming domain.^{18,28,29} More specifically, we have designed a set of nanoswitches displaying the same pH-responsive sequence containing 2 protonation centers (i.e., two cytosines) but differing in the length of the linker connecting the duplex portion to the triplex-forming domain (Figure 2a). The nanoswitches are labeled with a pH-insensitive fluorophore/quencher pair to follow pH-dependent folding/unfolding (Figure S11). Experiments performed at a fixed concentration of the nanoswitch and at different pH values show that the pH at which the triplex structure folds/unfolds is strongly correlated to the linker length. By shortening the length of the linker domain we observe a gradual increase of the pH value at which the triplex structure is destabilized (Figure 2b).

Received: April 28, 2019

Published: July 11, 2019

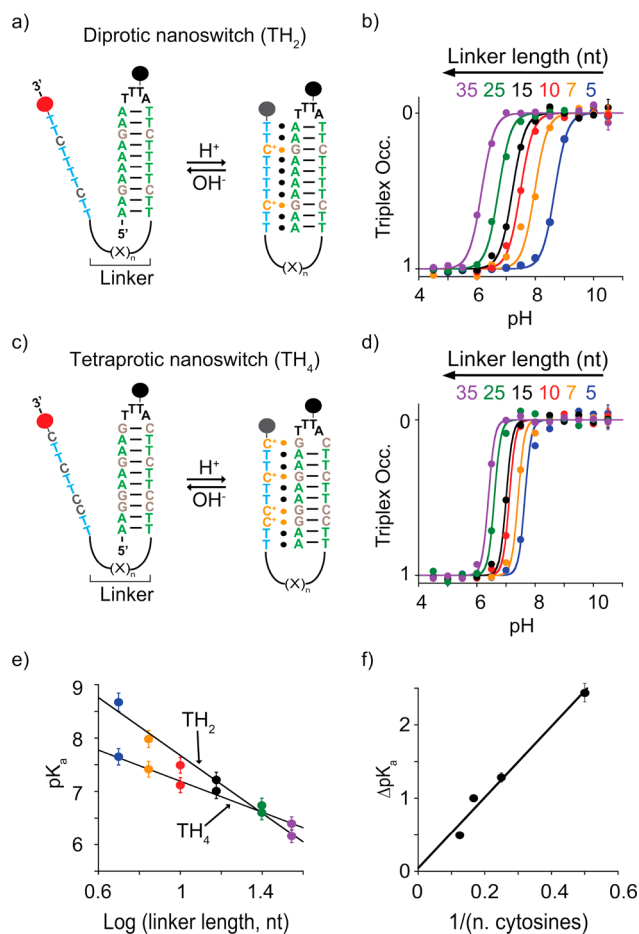


Figure 2. pH nanoswitches with rationally tailored pK_a . pH titration curves obtained with a set of diprotic, TH_2 (a,b) and tetraprotic, TH_4 (c,d) pH nanoswitches sharing the same pH-dependent triplex-forming domains and varying lengths of the linker domain. Solid lines in all pH curves represent fits obtained by nonlinear least-squares optimization with the equilibrium model outlined in the text. (e) pK_a vs $\log(\text{linker length, nt})$ for both the diprotic (TH_2) and tetraprotic (TH_4) nanoswitches. (f) ΔpK_a between the shortest and longest linkers (i.e., 5 and 35 nt) for different values of n (number of cytosines) vs $1/n$. The pH titration experiments were performed at 25 °C, $[\text{nanoswitch}] = 25$ nM by measuring the fluorescence signal at different pH values.³³

To better understand these experimental data, we developed a thermodynamic model that describes the pH-dependent triplex formation as a multistep process in which the n cytosines present in the single-stranded triplex-forming portion (S) are first protonated with an intrinsic acidity constant $K_{C(S)}$, presumably equal to that of free cytidine in aqueous solution ($pK_a = 4.08$),³⁰ followed by the intramolecular triplex (TH_n) formation characterized by the dimensionless intramolecular dissociation constant, K_d^{intra} . As a result, it is evidenced that the triplex behaves as a cooperative all-or-none n -protic acid whose cumulative acidity constant is given by $(K_{C(T)})^n$, where $K_{C(T)}$ is the average apparent acidity constant of a hydrogen bonded protonated cytosine in the triplex (see SI):



The cumulative acidity constant of the triplex is related to $K_{C(S)}$ and K_d^{intra} as shown by the following equation:

$$K_{C(T)}^n = K_d^{\text{intra}} K_{C(S)}^n = \frac{[S][H^+]^n}{[TH_n]} \quad (2)$$

Since at half-titration $pK_{C(T)} = \text{pH}$, the value of $pK_{C(T)}$ can be referred in common parlance as the pK_a of the switch:

$$pK_a = pK_{C(T)} = \frac{1}{n} pK_d^{\text{intra}} + pK_{C(S)} \quad (3)$$

Under a normalized fluorescent condition (0-1) in which only the duplex state is fluorescent, whereas the triplex state does not provide any signal, the following equation can be used to fit the experimental data by nonlinear least-squares:

$$F = \frac{K_a^n}{K_a^n + [H^+]^n} \quad (4)$$

The thermodynamic equilibrium model with $n = 2$ is able to describe the pH titration data very well for all linker lengths (Figure 2b, solid lines). The observed pK_a of the switch is modulated over more than 2 pH units (Figure 2b, Table S11). Indeed, by varying the length of the linker from 5 to 35 nucleotides, we can tune the observed pK_a from 8.7 ± 0.2 to 6.2 ± 0.2 , respectively.

To isolate the effect of the linker length on the overall stability of the complex, we employed the effective molarity, EM,³¹ defined as the ratio between the intermolecular dissociation constant between the triplex-forming portion and the duplex when the linker is absent, K_d^{inter} , and the intramolecular dissociation constant, K_d^{intra} , defined above:

$$EM = \frac{K_d^{\text{inter}}}{K_d^{\text{intra}}} \quad (5)$$

The EM is a measure of the propensity for an intramolecular process to occur relatively to the corresponding intermolecular process.³¹ Thus, while the EM only depends on the structural features of the linker, K_d^{inter} can vary with the sequence of the duplex portion and the single-stranded triplex-forming portion (i.e., number of cytosines). Substitution of eq 5 into eq 3 gives

$$pK_a = \frac{1}{n} \log EM + \frac{1}{n} pK_d^{\text{inter}} + pK_{C(S)} \quad (6)$$

In the case of entropic control of the effective molarity, a linear log-log correlation with a negative slope between EM and the linker length (number of nucleotides, nt) is expected.³² For a series of n -protic switches with the same n value, since pK_d^{inter} is constant, such a linear dependence would translate, according to eq 6, into a linear correlation with a negative slope between the pK_a of the switch and the log of linker length (straight line marked TH_2 , Figure 2e), thus confirming that the modulation of the pK_a is regulated solely by entropy through the EM parameter.

The modularity of the system employed in this work offers the opportunity to study how the modulation of pK_a is affected by the number of protonation centers in the triplex-forming portion of the switch. To this end, we have designed a new set of switches with the same linker lengths investigated above but with a single-stranded triplex-forming portion (S) containing four cytosines instead of the two employed before (Figure 2c). A linker dependent modulation of the pH value at which folding/unfolding of the triplex structure occurs is also observed in this case (see pK_a values in Table S12). However, from visual comparison of the pH titrations of the diprotic and tetraprotic switches (Figures 2b,d), some differences are

immediately apparent. As predicted by eq 4, the steepness of the titration curves increases on increasing the number n of available cytosines from 2 to 4. Moreover, the range of pK_a modulation upon increasing the linker length appears to be more restricted in the case of $n = 4$ compared to $n = 2$. This trend is clearly illustrated by the linear correlations of pK_a values against $\log(\text{linker length, nt})$ for the diprotic and tetraprotic switches (Figure 2e) which show a slope of -2.7 and -1.4 , respectively. The different slope is easily rationalized by the model embodied in eq 6, predicting that an increase of the number of protonation centers from $n = 2$ to $n = 4$, should decrease the slope by a factor of 2.

To further test the reliability of the proposed thermodynamic model, we have extended the study to the nanoswitches with $n = 6$ and $n = 8$, for the shortest (nt = 5) and longest (nt = 35) linkers (Table S13). These data allow to investigate how the ΔpK_a between the shortest and longest linkers (i.e., 5 and 35 nt), which represents the range of pK_a modulation, is affected by the number n of cytosines ($n = 2, 4, 6$, and 8). According to eq 6, for two nanoswitches of the same n value but different linker length, ΔpK_a is equal to $(1/n)\Delta(\log \text{EM})$. As a result, a plot of ΔpK_a vs $1/n$ should give a straight line passing through the origin, whose slope is $\Delta(\log \text{EM})$. The experimental data fit this prediction remarkably well (Figure 2f), thus strengthening our confidence in the proposed model. The meaning of the plot is straightforward: on increasing the number of cytosines (n) the pK_a of switches of different linker lengths converge to the same value. In other words, the entropy modulation achieved by varying the length of the linker is more and more dissipated by an increase of the number of protonation centers (i.e., cytosines). These same data also offer the possibility to understand how the number of cytosines might affect the intermolecular dissociation constant between the triplex-forming portion and the duplex when the linker is absent (i.e., pK_d^{inter}). As expected, the change in pK_d^{inter} observed by increasing the number of cytosines in the switch is indistinguishable, within error, between the switches with a 5 and 35 nt linker (see SI and Figure SI2). Moreover, the increase in pK_d^{inter} is remarkable (>11 units on passing from $n = 2$ to $n = 8$) further demonstrating the importance of the protonation of cytosines in the triplex formation.³⁴

To better understand the role of the linker length on the pK_a modulation of the switch, we have experimentally determined the entropic contribution for the different linker lengths through thermal melting curves and van't Hoff analysis at a fixed pH (5.5) for both the diprotic (Figure 3a,b) and tetraprotic (Figure 3c,d) switches.³⁵ We found that the melting temperature of all our nanoswitches scales linearly with the linker length (Figures SI3 and SI4). The length of the linker domains does not affect the enthalpic contribution of hydrogen bonding formation in triplex folding (see SI). The free energy values calculated through van't Hoff analysis with nanoswitches of different linker lengths can thus be used to obtain an estimate of the entropic contribution associated with the linker domain (ΔS_{linker}) by subtracting the ΔS value of the shortest linker (used as reference) to that of the other switches. As expected for a purely entropic controlled phenomenon, ΔS_{linker} scales linearly with the natural logarithm of the number of monomers (nucleotides) in the linker (Figure 3e),³² as well as with the pK_a of the corresponding switch (Figure 3f).

Finally, we observe a trend in the values of folding rate constants (k_f , s^{-1}) of the switches with different linker lengths with slower folding kinetics as the linker increases (Figures SI5

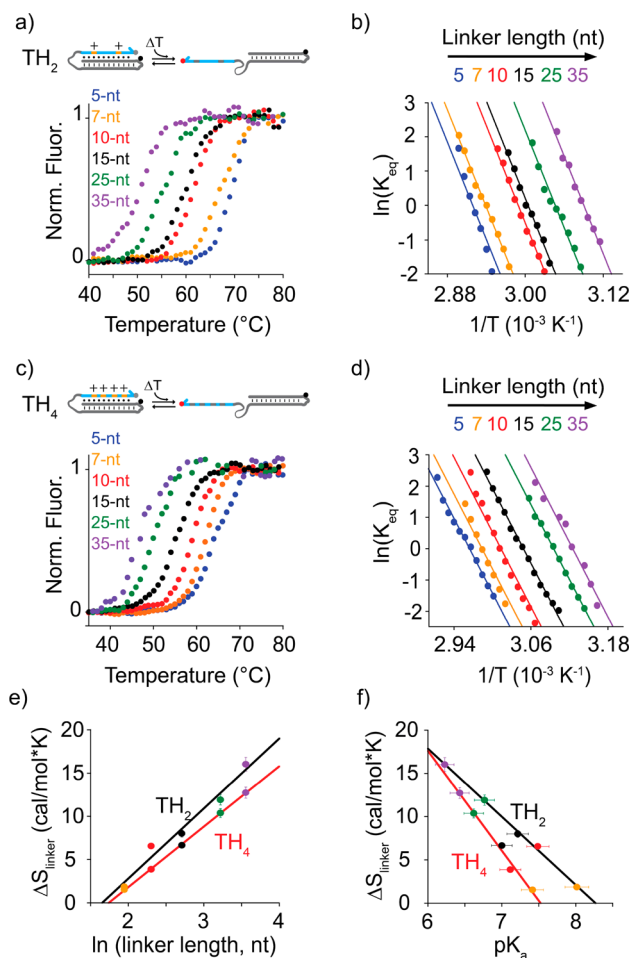


Figure 3. Thermodynamic characterization of the pH-dependent nanoswitches. Melting curve experiments and van't Hoff plots were used to measure the entropy associated with the linker domain. (a,b) Diprotic switches, TH₂; (c,d) tetraprotic switches, TH₄; (e,f) ΔS_{linker} values scale linearly with $\ln(\text{linker length, nt})$, and with pK_a values. The experimental values represent mean \pm s.d. of three separate measurements

and SI6). Conversely, because the unfolding process is not affected by the linker length, we do not observe any significant difference in the rate constants with different linker lengths (Figure SI7).

In conclusion, we have designed a family of multiprotic DNA-based pH-dependent nanoswitches that share the same hydrogen bond-forming domains but differ in the length of the linker connecting such domains. We have demonstrated that the modulation of the observed pK_a is due to a purely entropic contribution of the linker domain, which can be dissipated on increasing the number of protonation centers in the single-stranded triplex-forming portion.

This approach represents a highly versatile and predictable strategy to rationally modulate the pK_a of synthetic devices and might be used for a wide range of different applications, including the design of molecular machines and noncovalent assemblies with a finely tunable pH dependence. Compared to other strategies in which modulation of the pK_a of pH-dependent DNA-based nanoswitches has been achieved by modifying the pH-dependent domain^{18,36,37} or through allosteric control,³⁸ our approach appears advantageous because of the ease with which the entropy of single-stranded

DNA sequences can be gradually regulated. We also note that a similar strategy might be employed with other more complex biopolymers, including for example peptide sequences, thus allowing the rational design of synthetic protein-like biomolecular systems and assemblies^{39–42} with tunable pK_a values.

■ ASSOCIATED CONTENT

📄 Supporting Information

The Supporting Information is available free of charge on the ACS Publications website at DOI: 10.1021/jacs.9b04168.

Experimental, thermodynamic model and data analysis, thermodynamic analysis of thermal melting curves, supporting figures (PDF)

■ AUTHOR INFORMATION

Corresponding Author

*francesco.ricci@uniroma2.it

ORCID

Davide Mariottini: 0000-0001-6121-6428

Andrea Idili: 0000-0002-6004-270X

Gianfranco Ercolani: 0000-0003-2437-3429

Francesco Ricci: 0000-0003-4941-8646

Notes

The authors declare no competing financial interest.

■ ACKNOWLEDGMENTS

This work was supported by the European Research Council, ERC (project no. 336493, FR), by Associazione Italiana per la Ricerca sul Cancro, AIRC (project no. 21965, FR) and by the Italian Ministry of Health (project no. GR-2013-02356714).

■ REFERENCES

- (1) Masureel, M.; Martens, C.; Stein, R. A.; Mishra, S.; Ruyschaert, J.-M.; Mchaourab, H. S.; Govaerts, C. Protonation drives the conformational switch in the multidrug transporter LmrP. *Nat. Chem. Biol.* **2014**, *10*, 149–155.
- (2) Sharif, S.; Schagen, D.; Toney, M. D.; Limbach, H.-H. Coupling of Functional Hydrogen Bonds in Pyridoxal-5'-phosphate–Enzyme Model Systems Observed by Solid-State NMR Spectroscopy. *J. Am. Chem. Soc.* **2007**, *129*, 4440–4455.
- (3) Šponer, J.; Leszczynski, J.; Hobza, P. Electronic properties, hydrogen bonding, stacking, and cation binding of DNA and RNA bases. *Biopolymers* **2001**, *61*, 3–31.
- (4) Fonseca Guerra, C.; Bickelhaupt, F. M.; Snijders, J. G.; Baerends, E. J. Hydrogen Bonding in DNA Base Pairs: Reconciliation of Theory and Experiment. *J. Am. Chem. Soc.* **2000**, *122*, 4117–4128.
- (5) Baker, E. N.; Hubbard, R. E. Hydrogen bonding in globular proteins. *Prog. Biophys. Mol. Biol.* **1984**, *44*, 97–179.
- (6) Yang, S. K.; Zimmerman, S. C. Hydrogen Bonding Modules for Use in Supramolecular Polymers. *Isr. J. Chem.* **2013**, *53*, 511–520.
- (7) Isom, D. G.; Castañeda, C. A.; Cannon, B. R.; García-Moreno, E. B. Large shifts in pK_a values of lysine residues buried inside a protein. *Proc. Natl. Acad. Sci. U. S. A.* **2011**, *108*, 5260–5265.
- (8) Prins, L. J.; Reinhoudt, D. N.; Timmerman, P. Noncovalent Synthesis Using Hydrogen Bonding. *Angew. Chem., Int. Ed.* **2001**, *40*, 2382–2426.
- (9) Seto, T. C.; Mathias, J. P.; Whitesides, G. M. Molecular self-assembly through hydrogen bonding: aggregation of five molecules to form a discrete supramolecular structure. *J. Am. Chem. Soc.* **1993**, *115*, 1321–1329.
- (10) De Greef, T. F. A.; Smulders, M. M.; Wolffs, M.; Schenning, A. P.; Sijbesma, R. P.; Meijer, E. W. Supramolecular Polymerization. *Chem. Rev.* **2009**, *109*, 5687–5754.

(11) Fathalla, M.; Lawrence, C. M.; Zhang, N.; Sessler, J. L.; Jayawickramarajah, J. Jayawickramarajah, Base-pairing mediated non-covalent polymers. *Chem. Soc. Rev.* **2009**, *38*, 1608–1620.

(12) De Greef, T. F. A.; Meijer, E. W. Materials science: supramolecular polymers. *Nature* **2008**, *453*, 171–173.

(13) Blight, B. A.; Hunter, C. A.; Leigh, D. A.; McNab, H.; Thomson, P. I. T. An AAAA–DDDD quadruple hydrogen-bond array. *Nat. Chem.* **2011**, *3*, 244–248.

(14) Leigh, D. A.; Wong, J. K. Y.; Dehez, F.; Zerbetto, F. Unidirectional rotation in a mechanically interlocked molecular rotor. *Nature* **2003**, *424*, 174–179.

(15) Altieri, A.; Bottari, G.; Dehez, F.; Leigh, D. A.; Wong, J. K. Y.; Zerbetto, F. Remarkable Positional Discrimination in Bistable Light- and Heat-Switchable Hydrogen-Bonded Molecular Shuttles. *Angew. Chem., Int. Ed.* **2003**, *42*, 2296–2300.

(16) Gatti, G. F.; Leigh, D. A.; Nepogodiev, S. A.; Slawin, A. M. Z.; Teat, S. J.; Wong, J. K. Y. Stiff, and Sticky in the Right Places: The Dramatic Influence of Preorganizing Guest Binding Sites on the Hydrogen Bond-Directed Assembly of Rotaxanes. *J. Am. Chem. Soc.* **2001**, *123*, 5983–5989.

(17) Gatti, G. F.; León, S.; Wong, J. K. Y.; Bottari, G.; Altieri, A.; Farran Morales, M. A.; Teat, S. J.; Frochot, C.; Leigh, D. A.; Brouwer, A. M.; Zerbetto, F. Photoisomerization of a rotaxane hydrogen bonding template: Light-induced acceleration of a large amplitude rotational motion. *Proc. Natl. Acad. Sci. U. S. A.* **2003**, *100*, 10–14.

(18) Idili, A.; Vallée-Bélisle, A.; Ricci, F. Programmable pH-Triggered DNA Nanoswitches. *J. Am. Chem. Soc.* **2014**, *136*, 5836–5839.

(19) Modi, S.; Nizak, C.; Surana, S.; Halder, S.; Krishnan, Y. Two DNA nanomachines map pH changes along intersecting endocytic pathways inside the same cell. *Nat. Nanotechnol.* **2013**, *8*, 459–467.

(20) Narayanaswamy, N.; Chakraborty, K.; Saminathan, A.; Zeichner, E.; Leung, K. H.; Devany, J.; Krishnan, Y. A pH-correctable, DNA-based fluorescent reporter for organellar calcium. *Nat. Methods* **2019**, *16*, 95–102.

(21) Modi, S.; Swetha, M. G.; Goswami, D.; Gupta, G. D.; Mayor, S.; Krishnan, Y. A DNA nanomachine that maps spatial and temporal pH changes inside living cells. *Nat. Nanotechnol.* **2009**, *4*, 325–330.

(22) Kawai, S. H.; Gilat, S. L.; Lehn, J.-M. Photochemical pK_a-Modulation and Gated Photochromic Properties of a Novel Diarylethene Switch. *Eur. J. Org. Chem.* **1999**, *1999*, 2359–2366.

(23) Ragazzon, G.; Schäfer, C.; Franchi, P.; Silvi, S.; Colasson, B.; Lucarini, M.; Credi, A. Remote electrochemical modulation of pK_a in a rotaxane by co-conformational allostery. *Proc. Natl. Acad. Sci. U. S. A.* **2018**, *115*, 9385–9390.

(24) Ghosh, I.; Nau, W. M. The strategic use of supramolecular pK(a) shifts to enhance the bioavailability of drugs. *Adv. Drug Delivery Rev.* **2012**, *64*, 764–783.

(25) (a) Vallée-Bélisle, A.; Plaxco, K. W. Structure-switching biosensors: inspired by Nature. *Curr. Opin. Struct. Biol.* **2010**, *20*, 518–526. (b) Pardee, K.; Green, A. A.; Takahashi, M. K.; Braff, D.; Lambert, G.; Lee, J. W.; Ferrante, T.; Ma, D.; Donghia, N.; Fan, M.; Daringer, N. M.; Bosch, I.; Dudley, D. M.; O'Connor, D. H.; Gehrke, L.; Collins, J. J. Rapid Low-Cost Detection of Zika Virus Using Programmable Biomolecular Components. *Cell* **2016**, *165*, 1255–1266.

(26) Ricci, F.; Vallée-Bélisle, A.; Simon, A. J.; Porchetta, A.; Plaxco, K. W. Using Nature's "Tricks" To Rationally Tune the Binding Properties of Biomolecular Receptors. *Acc. Chem. Res.* **2016**, *49*, 1884–1892.

(27) Lin, M.; Song, P.; Zhou, G.; Zuo, X.; Aldalbahi, A.; Lou, X.; Shi, J.; Fan, C. Electrochemical detection of nucleic acids, proteins, small molecules and cells using a DNA-nanostructure-based universal biosensing platform. *Nat. Protoc.* **2016**, *11*, 1244–1263.

(28) Porchetta, A.; Idili, A.; Vallée-Bélisle, A.; Ricci, F. General Strategy to Introduce pH-Induced Allostery in DNA-Based Receptors to Achieve Controlled Release of Ligands. *Nano Lett.* **2015**, *15*, 4467–4471.

(29) Hu, Y.; Ceconello, A.; Idili, A.; Ricci, F.; Willner, I. Triplex DNA Nanostructures: From Basic Properties to Applications. *Angew. Chem., Int. Ed.* **2017**, *56*, 15210–15233.

(30) Christensen, J. J.; Rytting, J. H.; Izatt, R. M. Thermodynamics of proton dissociation in dilute aqueous solution. VII. *J. Phys. Chem.* **1967**, *71*, 2700–2705.

(31) Di Stefano, S.; Ercolani, G. Chapter One - Equilibrium Effective Molarity As a Key Concept in Ring-Chain Equilibria, Dynamic Combinatorial Chemistry, Cooperativity and Self-assembly. *Adv. Phys. Org. Chem.* **2016**, *50*, 1–76.

(32) Jacobson, H.; Stockmayer, W. H. Intramolecular Reaction in Polycondensations. I. The Theory of Linear Systems. *J. Chem. Phys.* **1950**, *18*, 1600–1606.

(33) Error bars in the titration curves are depicted for only one point on each curve and represent the typical standard deviations obtained on at least three independent measurements.

(34) Asensio, J. L.; Lane, A. N.; Dhesi, J.; Bergqvist, S.; Brown, T. The contribution of cytosine protonation to the stability of parallel DNA triple helices. *J. Mol. Biol.* **1998**, *275*, 811–822.

(35) Mergny, J.-L.; Lacroix, L. Analysis of thermal melting curves. *Oligonucleotides* **2003**, *13*, 515–537.

(36) Halder, S.; Krishnan, Y. Design of ultrasensitive DNA-based fluorescent pH sensitive nanodevices. *Nanoscale* **2015**, *7*, 10008–10012.

(37) Lannes, L.; Halder, S.; Krishnan, Y.; Schwalbe, H. Tuning the pH Response of i-Motif DNA Oligonucleotides. *ChemBioChem* **2015**, *16*, 1647–1656.

(38) Nesterova, I. V.; Nesterov, E. E. Rational Design of Highly Responsive pH Sensors Based on DNA i-Motif. *J. Am. Chem. Soc.* **2014**, *136*, 8843–8846.

(39) Fleming, S.; Ulijn, R. V. Design of nanostructures based on aromatic peptide amphiphiles. *Chem. Soc. Rev.* **2014**, *43*, 8150–8177.

(40) Hirst, A. R.; Roy, S.; Arora, M.; Das, A. K.; Hodson, N.; Murray, P.; Marshall, S.; Javid, N.; Sefcik, J.; Boekhoven, J.; van Esch, J. H.; Santabarbara, S.; Hunt, N. T.; Ulijn, R. V. Biocatalytic induction of supramolecular order. *Nat. Chem.* **2010**, *2*, 1089–1094.

(41) Pappas, C. G.; Shafi, R.; Sasselli, I. R.; Siccardi, H.; Wang, T.; Narang, V.; Abzalimov, R.; Wijerathne, N.; Ulijn, R. Dynamic peptide libraries for the discovery of supramolecular nanomaterials. *Nat. Nanotechnol.* **2016**, *11*, 960–967.

(42) Gazit, E. Self-assembled peptide nanostructures: the design of molecular building blocks and their technological utilization. *Chem. Soc. Rev.* **2007**, *36*, 1263–1269.